N_2O decomposition over $(CaO)_{1-x}(MO)_x$ oxide systems (M = Ti, Cr): relation with photoluminescence

Loukia A. Loukatzikou,* Antonios T. Sdoukos and Philip J. Pomonis

Department of Chemistry, University of Ioannina, Ioannina 45110, Greece

$(CaO)_{1-x}(MO)_x$ oxide systems (M = Ti, Cr; $x = 0$–1), prepared at 1150 °C under atmospheric conditions, were investigated for their photoluminescence as well as for their catalytic activity in N_2O decomposition in the temperature range 400–650 °C. As shown by XRD analysis, the solids are either multicomponent systems or simple phase oxides. Titanium addition to CaO of up to 30% results in a significant enhancement of the catalytic activity, while chromium addition beyond 1% has the reverse effect; solids rich in Ti or Cr are rather inactive. Thus, the systems showing considerable activity are either simple phase CaO, or CaO–$CaTiO_3$ mixed oxides. The photoluminescence intensity of the catalysts was found to be suppressed by addition of Cr or Ti (> 0.5%) to CaO. Although the catalytic activity is affected in different ways by addition of Ti or Cr, and a variety of structural composition are noted for the $(CaO)_{1-x}(MO)_x$ catalysts, a relation between catalytic activity and photoluminescence is observed, not only across each sample series, but also for the total set of catalysts.

In view of its relative simplicity, N_2O decomposition has been extensively chosen as a probe reaction, to investigate the catalytic properties of various oxide system surfaces.[1–7] Electron-transfer processes between the catalytic surface and the reactants and/or the products are known to have to be significant for the reaction to proceed. Thus, this reaction has been frequently used in evaluating the effects of not only the physicochemical, but also of the electronic properties of solids on catalytic activity.

Recently, we have found that the catalytic activity of $(CaO)_{1-x}(ZnO)_x$ mixed oxides for N_2O decomposition is related linearly to the photoluminescence intensity of the oxides.[8] The luminescence of the above solids, produced by means of high UV energy excitation, is a result possibly of recombination processes between photogenerated electrons and holes, according to the simplified model proposed in ref. 9. If so, the above mentioned relationship, indicating a similarity between the catalytic and luminescence processes, could be also revealing for the photocatalytic N_2O elimination mechanism over those solids.[8]

It is of interest to investigate the influence of some 3d ions added to CaO, other than the filled band ($3d^{10}$) Zn^{2+}, on the catalytic as well as the photoluminescence behaviour of the solids and also to look for a possible relation between these parameters. The present work aims to search for such a possible influence for the unfilled band Ti^{4+} ions ($3d^0$), as well as for the partially filled band Cr^{5+} ($3d^1$) or Cr^{3+} ($3d^3$) ions. This is attempted by studying two series of specimens prepared by solid-state reactions, *viz.* $(CaO)_{1-x}(MO)_x$, where M = Ti or Cr and $x = 0$–1.

Experimental

Polycrystalline $(CaO)_{1-x}(MO)_x$ (M = Ti or Cr; $x = 0.000$, 0.005, 0.010, 0.050, 0.100, 0.300, 0.500, 0.700, 0.900, 0.950, 0.995 or 1.000) powders were prepared by firing intimate mixtures of CaO (Fluka, p.a) and TiO_2 (Griffin, c. r.) or $Cr(NO_3)_3 \cdot 9H_2O$ (Fluka, p.a). The starting materials were mixed and ground thoroughly before firing in air for 5 h at 1150 °C. This procedure was repeated three times. Then, the solids were left to cool slowly at room temperature, in order to obtain the hydroxylated oxide precursors. As shown by thermogravimetry experiments, the latter are converted completely into oxides after heating at 650 °C in an He flow for 30 min. A different pretreatment was followed in order to obtain the $(CaO)_{1-x}(MO)_x$ oxides for XRD, as well as for photoluminescence measurements: the solids were quickly removed from the 400 °C furnace after high-temperature treatment, and were ground and stored in glass vials. Thermal analysis showed that neither $Ca(OH)_2$ nor $CaCO_3$ were detectable from the solids treated as described above. The oxides are designated as CM : y where M is Ti or Cr and y is the percentage of M atoms relative to the total amount of metal (Ca + M) atoms in the sample [$y = 100$ M/(Ca + M); Table 1].

The N_2O decomposition reaction was carried out in the dark, in a bench-scale plug-flow reactor (PFR) similar to that described in ref. 8 and 10. Helium–N_2O (2 : 1) at a flow rate of 75 cm^3 min^{-1} was allowed to flow through the reactor, consisting of a silica tube of 1 cm diameter with a perforated glass bed, on which 0.2 g of the solid was placed. A Varian 3700 gas chromatograph equipped with a TCD was used to analyse both reactants and products. The catalytic activity of the oxides was measured *in situ* in the catalytic reactor, after calcination for 30 min of their precursors at 650 °C in flowing helium. The temperature range examined was 400–650 °C. In each experiment the reaction rate was calculated as the amount reacted per unit mass of the catalyst.

X-Ray diffraction (XRD) patterns of the prepared oxides were obtained in a Philips system (PW 2253 lamp, PW 1050 goniometer, PW 1965/50 analogue detector) using Cu-Kα radiation ($\lambda = 1.542$ Å).

The photoluminescence of the solids was recorded at room temperature in air, using a Perkin Elmer LS-3 fluorescence spectrometer equipped with a 150 W xenon lamp and a side-window photomultiplier tube (EMI 9781 RA) and details are given elsewhere.[9] The excitation spectra were corrected for the source intensity as well as for the excitation monochromator efficiency, however, the emission spectra were not corrected for the photomultiplier response. The spectral band maxima were identified by point-to-point measurements of the luminescence intensity *vs.* wavelength in the range of interest.

Results

XRD

The crystal phases detected by XRD and dominant over the various samples CTi : y and CCr : y solids are shown in Table 1. The samples with $y = 0.5$–1 and 99–99.5 represent simple phase CaO and TiO_2 or Cr_2O_3 oxides, respectively. The remainder

Table 1 Designation of the $(CaO)_{1-x}(MO)_x$ solids and the crystal phases detected by XRD; M denotes the metal ions present (Ti or Cr)

x	designation	Ti			Cr		
0.00	CM : 0.00	CaO	—	—	CaO	—	—
0.005	CM : 0.5	CaO	—	—	CaO	—	—
0.01	CM : 1	CaO	—	—	CaO	—	—
0.05	CM : 5	CaO[a]	$CaTiO_3$	—	CaO[a]	$Ca_5(CrO_4)_3OH$	—
0.10	CM : 10	CaO[a]	$CaTiO_3$	—	CaO[a]	$Ca_5(CrO_4)_3OH$	—
0.30	CM : 30	CaO[a]	$CaTiO_3$	TiO_2	CaO[a]	$Ca_5(CrO_4)_3OH$	—
0.50	CM : 50	CaO	$CaTiO_3$[a]	TiO_2	—	$Ca_5(CrO_4)_3OH$	Cr_2O_3[a]
0.70	CM : 70	CaO	$CaTiO_3$[a]	TiO_2	—	$Ca_5(CrO_4)_3OH$	Cr_2O_3[a]
0.90	CM : 90	—	$CaTiO_3$	TiO_2[a]	—	$Ca_5(CrO_4)_3OH$	Cr_2O_3[a]
0.95	CM : 95	—	$CaTiO_3$	TiO_2[a]	—	$Ca_5(CrO_4)_3OH$	Cr_2O_3[a]
0.99	CM : 99	—	—	TiO_2	—	—	Cr_2O_3
0.995	CM : 99.5	—	—	TiO_2	—	—	Cr_2O_3
1.00	CM : 100	—	—	TiO_2	—	—	Cr_2O_3

[a]Predominant phase.

of the samples ($y \neq 0$, 100) are multicomponent, *e.g* mixtures of two or three simple phases in varying ratios. Except for the three simple oxides, cubic CaO, tetragonal TiO_2 (rutile) and hexagonal Cr_2O_3, orthorhombic $CaTiO_3$ and hexagonal $Ca_5(CrO_4)_3(OH)$ phases were detected within the two series of samples.

Photoluminescence spectra

The emission spectra of CTi : *y* and CCr : *y* solids excited at 200, 220 and 240 nm are shown in Fig. 1 and 2, respectively. In general, broad emission bands in the 300–650 nm region were recorded, consisting of three overlapping components peaking in the visible range of the spectra.

The similarity in the spectral features of the CTi : *y* solids as a whole is clear (Fig. 1), although some differences are observed in the relative band intensities, as well as minor changes in the energy maxima. Excitation of CTi : *y* solids in the region 200–220 nm results mainly in blue ($\lambda_{max} = 429$–444 nm) or

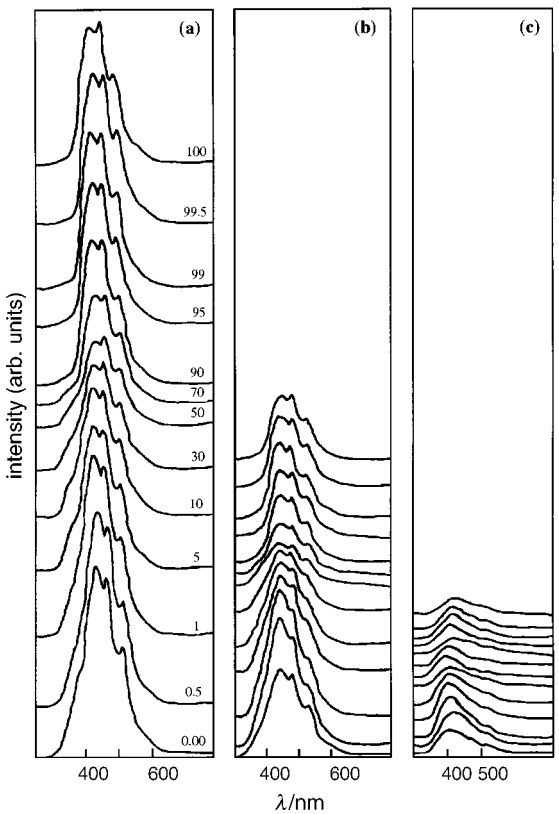

Fig. 1 Emission spectra of CTi : *y* solids. (a) $\lambda_{ex} = 200$ nm, (b) $\lambda_{ex} = 220$ nm, (c) $\lambda_{ex} = 240$ nm (values of *y* are given on the figure).

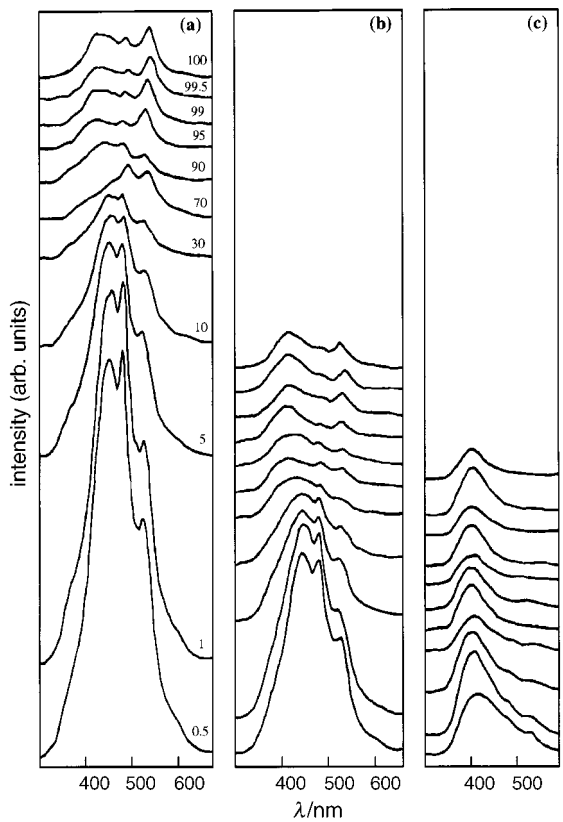

Fig. 2 Emission spectra of CCr : *y* solids. (a) $\lambda_{ex} = 200$ nm, (b) $\lambda_{ex} = 220$ nm, (c) $\lambda_{ex} = 240$ nm.

blue–green ($\lambda_{max} = 463$–484 nm) emission, depending on the sample, while a third band also appears at the green region of the spectra ($\lambda_{max} = 508$–534 nm). However, a main violet emission ($\lambda_{max} = 404$–427 nm) is produced with 240 nm excitation of all the CTi : *y* solids and emission components at longer wavelengths are recorded as shoulders of the main violet band.

Blue ($\lambda_{max} = 436$–452 nm) or blue–green ($\lambda_{max} = 472$–486 nm) emission is also the main feature in the spectra of CCr : 0.5–90 solids, although green emission ($\lambda_{max} = 517$–532 nm) dominates for the other CCr : *y* solids, produced by excitation at 200 nm. By contrast, excitation of CCr : *y* ($y = 0.5$–100) solids at 220 or 240 nm results mainly in blue ($\lambda_{max} = 408$–448 nm) or violet ($\lambda_{max} = 400$–410 nm) emission, respectively.

The excitation spectra of the CTi : *y* and CCr : *y* samples are shown in Fig. 3 and 4, respectively. All the excitation spectra of the CTi : *y* solids, recorded for an emission wavelength of 430, 470 or 510 nm, show a broad band with a maximum at 200–207 nm as well as a second weak band at 224–240 nm.

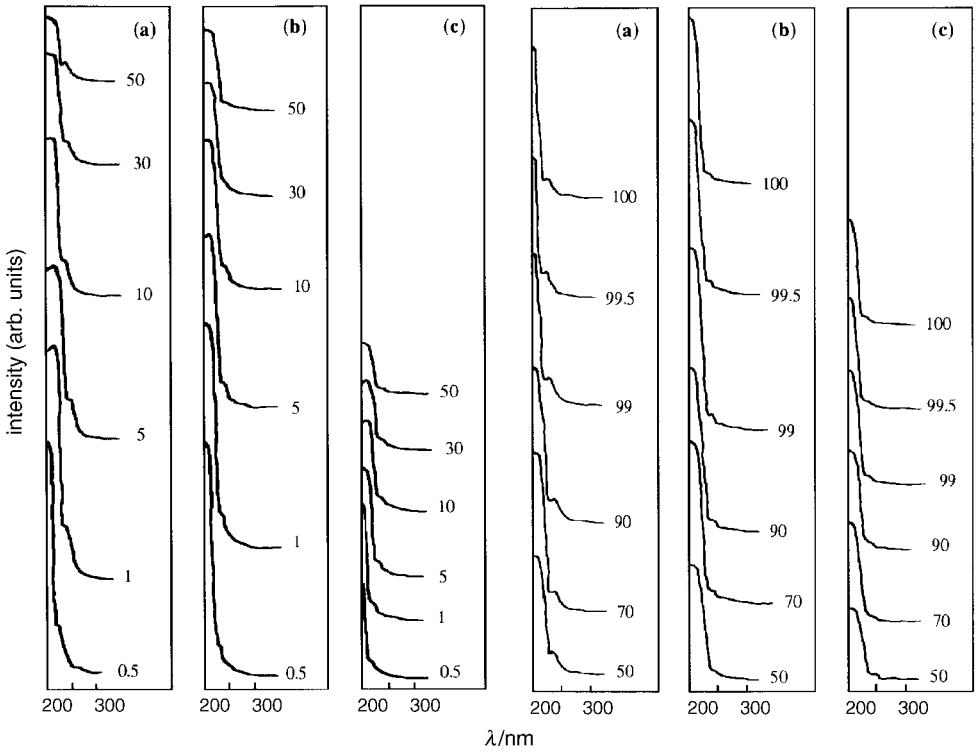

Fig. 3 Excitation spectra of CTi:y solids. (a) $\lambda_{em}=430$ nm, (b) $\lambda_{em}=470$ nm, (c) $\lambda_{em}=510$ nm.

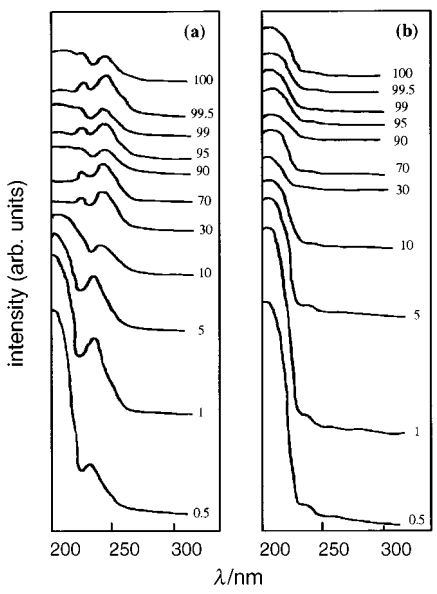

Fig. 4 Excitation spectra of CCr:y solids. (a) $\lambda_{em}=410$ nm, (b) $\lambda_{em}=525$ nm.

The green ($\lambda=525$ nm) emission of the CCr:y solids arise also from the main excitation band at 200–206 nm and from the second, very weak excitation band at 232–237 nm [Fig. 4(b)], as in the case of the CTi:y solids. Similarly, the emission at 410 nm is the result of two excitation states, the main state at 200–206 nm and a second at 232–240 nm, for CCr:0.5–10 solids, but for CCr:30–100 solids [Fig. 4(a)] this is also the result of a third excitation state, at 219–223 nm. The excitation spectrum of CCr:30–100 solids is very weak (Fig. 4), therefore the contribution of each excitation state is now almost the same.

The blue ($\lambda_{max}=428$–452 nm) emission intensity, produced by excitation at 200 nm, varies across the $(CaO)_{1-x}(MO)_x$ (M = Ti, Cr) solids as shown in Fig. 5(a) and (b). The luminescence intensity of the solids containing titanium decreased logarithmically with increase in x from 0.005 to 0.5, but thereafter ($x=0.5$–1) appears to increase again [Fig. 5(a)]. A logarithmic diminution of the luminescence intensity is also observed with increase in x from 0.005–0.3 for solids containing chromium, but at $x=0.3$–1 it remains at the same, albeit at a very weak level [Fig. 5(b)].

Catalytic tests

The catalytic activities of CM:y (M = Ti, Cr) solids for N_2O decomposition are shown in Table 2 in the form R (mol g^{-1} s^{-1}) for various temperatures. All the Ca-rich samples as well as the isomolecular CTi:y samples are more active than pure CaO; CTi:70 shows only low activity, while the remainder Ca-poor series are rather inactive for the reaction. On the other hand, only samples rich in Ca ($y=0.5$–30) are active for the N_2O decomposition across the CCr:y series, those with $y=0.5$–1 are especially more active than pure CaO.

The activation energies for the N_2O decomposition were determined following the statistical treatment of the relevant rate equations as was done previously.[10–12] Briefly, the kinetics of the reaction has been analysed taking into consideration the equation for a plug-flow reactor:

$$F\mathrm{d}x = R\mathrm{d}m \quad (1)$$

where F is the reactor feed in N_2O (mol s^{-1}), x the degree of conversion, R the reaction rate and m the mass of the catalyst used (0.2 g), as well as the following three equations:

$$R = kb_{N_2O}P_{N_2O} \quad (2)$$

$$R = k \quad (3)$$

$$R = kb_{N_2O}P_{N_2O}/(b_{O_2}P_{O_2})^{1/2} \quad (4)$$

where b and P represent the corresponding adsorption coefficients and partial pressures of the species indicated. The above kinetic expressions are based on Langmuir adsorption isotherms as usually done in similar cases for N_2O

Table 2 Reaction rate (mol $g^{-1}s^{-1}$) for N_2O decomposition over the CTi : *y* and CCr : *y* solids at various temperatures

	$R/10^{-5}$ mol g^{-1} s^{-1}					
sample	400 °C	450 °C	500 °C	550 °C	600 °C	650 °C
CaO	—	0.297	1.023	2.743	5.506	—
CTi : 0.5	0.846	1.228	4.315	7.905	—	—
1	0.177	1.265	4.389	8.333	—	—
5	0.205	1.367	4.845	8.305	—	—
10	—	0.763	2.948	6.175	8.463	—
30	0.074	0.512	2.139	5.933	8.184	—
50	—	0.325	1.525	4.287	7.403	—
70	—	—	—	0.790	2.195	4.064
90	—	—	—	—	0.121	0.307
95	—	—	—	—	—	0.065
99	—	—	—	—	—	0.046
99.5	—	—	—	—	—	0.046
TiO_2	—	—	—	—	—	0.121
CCr : 0.5	—	0.344	1.637	4.520	6.705	—
1	—	0.437	1.953	4.752	7.691	—
5	—	—	0.642	1.999	4.064	6.603
10	—	—	—	0.986	2.399	5.357
30	—	—	—	0.800	2.027	4.176
50	—	—	—	—	—	0.074
70	—	—	—	—	—	0.074
90	—	—	—	—	—	0.149
95	—	—	—	—	—	0.074
99	—	—	—	—	—	0.139
99.5	—	—	—	—	—	0.205
Cr_2O_3	—	—	—	—	—	0.130

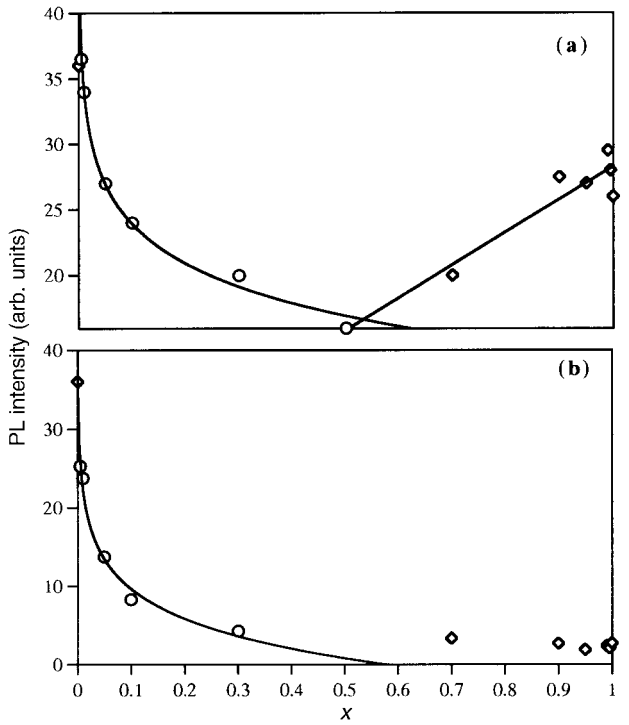

Fig. 5 Photoluminescence intensity of the $(CaO)_{1-x}(MO)_x$ solids *vs.* metal content *x*. (a) M = Ti, (b) M = Cr (λ_{ex} = 200 nm).

adsorption.[10–14] Such adsorption isotherms can be differentiated according to three extreme cases concerning the adsorption of reactants and products: (*i*) weak adsorption of both N_2O and O_2 [eqn. (2)], (*ii*) strong adsorption of N_2O and weak adsorption of O_2 [eqn. (3)], and (*iii*) strong adsorption of O_2 and weak adsorption of N_2O [eqn. (4)].

The experimental data were analysed using the integrated form of eqn. (2), which was found to fit best in all cases. We note that the eqn. (2)–(4) can be properly transformed to linear equations by taking also into account our experimental conditions.[10–12] The rate equation applied in each case was selected by testing the minimum percentage standard errors and the maximum correlation coefficient determined by linear regression. The apparent activation energies E_a as well as the pre-exponential factors ln *A* calculated in this manner are listed in Table 3.

The N_2O decomposition reaction is known to proceed on oxides, solid solutions and perovskites, through the following steps.[1,2,10,13,14]

$$N_2O_{(g)} + S \rightarrow N_2O^-_{(ads)} + S^+ \quad \text{(I)}$$

$$N_2O^-_{(ads)} \rightarrow N_{2(g)} + O^-_{(ads)} \quad \text{(II)}$$

$$2O^-_{(ads)} + 2S^+ \rightarrow O_{2(g)} + 2S \quad \text{(III)}$$

or

$$O^-_{(ads)} + N_2O_{(g)} + S^+ \rightarrow N_{2(g)} + O_{2(g)} + S \quad \text{(IV)}$$

where S represents a catalytic surface site, while (g) and (ads) indicate the gas and adsorbed state respectively. Step (I) involves the activation of N_2O by electron donation from the catalytic surface and the generation of an electron-deficient site (S^+). Steps (III) and (IV) represent the O_2 desorption, which should proceed by electron release back to the catalyst. Strong adsorption of oxygen on the catalytic surface signifies strong inhibition of the reaction by oxygen.

The fact that the N_2O decomposition obeys the rate equation (2) in all cases examined, implies there is no inhibition by the oxygen here but that the N_2O activation on the surfaces is very important.[14] Therefore, the rate controlling step is the activated adsorption of N_2O on the catalytic surface (step I).

Discussion

Relation between catalytic activity and XRD phases

The appearance of the catalytic activity should be somehow correlated to the XRD phases detected across the CM : *y* (M = Ti, Cr) catalysts. Comparison of the experimental data given in Tables 1 and 2 shows that the active CaO phase is dominant, if not the only phase detected by XRD for the CM : 0.5–30, (M = Ti, Cr) catalysts. The $CaTiO_3$ phase should also be active, since it is the second phase detected in the active CTi : 5–10 mixed oxides and the dominant phase in the CTi : 50–70 solids, which also exhibit some activity. The gradual decrease of the catalytic activity across the CTi : 30–70 catalysts is probably the result of the gradually increased presence of the TiO_2 phase, which appears to poison the catalyst. The tetragonal rutile form of TiO_2, as well as the hexagonal Cr_2O_3 phase, were found to be inactive for N_2O activation under our experimental conditions. The hexagonal $Ca_5(CrO_4)_3(OH)$ phase appears also to poison the catalytically active CaO, since its increased presence is accompanied by a considerable decrease in the catalytic activity across the CCr : 5–30 solids, to below that of pure CaO. Therefore, the oxide systems

Table 3 Arrhenius parameters for the CM : *y* (M = Ti, Cr) catalysts

catalyst	E_a/kJ mol^{-1}	ln *A*
CaO	116.85	18.06
CTi : 0.5	120.36	20.24
1	154.42	25.55
5	135.07	22.64
10	114.22	18.72
30	125.27	20.16
50	131.24	20.66
70	116.54	16.72
CCr : 0.5	122.95	19.40
1	126.59	20.13
5	110.06	16.63
10	126.01	18.27
30	118.03	16.92

showing considerable activity are either simple phase CaO, or $CaO–CaTiO_3$ mixed oxides.

Photoluminescence spectra

The luminescence spectra of TiO_2 in air recorded under high-energy UV excitation (Figs. 1, 3) are different from spectra of the oxide in the rutile form reported in the literature,[15–18] although similar emissions have been observed. Free exciton emission has been observed at low temperatures from rutile single crystals,[15,16] but the emission recorded from rutile powders at 77 K,[18] consists of a broad band at 450–550 nm with a maximum at *ca.* 500 nm. The latter band was found to be quenched by O_2 or N_2O and to be enhanced by addition of H_2O or H_2.[18] A quite similar emission has been obtained from small particles of TiO_2, which also has been found to be quenched by molecular oxygen and seems to be associated with the presence of adsorbed H_2O and/or the surface OH^- groups.[17] The green emission band ($\lambda_{max} = 510–530$ nm) recorded here from TiO_2 in air (Fig. 1) coexists with distinct emission components at higher energies. Besides, a similar green emission is also recorded from all of the CTi:*y* solids, including pure CaO. Thus, the origin of the rutile luminescence recorded here seems to be different from that reported in the literature.

We stress the point that the luminescence of TiO_2 produced by high-energy UV excitation (5.2–6.2 eV) is intense and visible to the naked eye, while excitation of rutile powders at *ca.* 300 nm at room temperature results in very low luminescence yields.[18] No photoluminescence was found from TiO_2 at 300–340 nm excitation, in accord with the literature data.[18] In general, the luminescence of TiO_2 in the rutile form reported in the literature has been observed at low temperatures, following excitation with energy a little greater than the band gap of the oxide.[15–18] Therefore, the marked differences above in the TiO_2 luminescence spectra are due to the different excitation energies used rather than differences in sample treatment methods.

On the other hand, the luminescence spectra of TiO_2 in air are similar to the corresponding CaO spectra (Figs. 1, 3). A similarity is also clear between the spectral features of the pure oxides and those of the multicomponent CTi:*y* solids as a whole. We note that the $CaTiO_3$ crystal phase was detected by XRD for the CTi:5–95 solids. Although $CaTiO_3$ has been reported to luminesce with an emission maximum at 445 nm,[19] *i.e.* near the high-energy emission band component in the spectra of the above solids, its presence does not seem to be the cause of the latter, since this emission is present in all the spectra of the CTi:*y* solids, independent of their $CaTiO_3$ content. Also, the emission of $CaTiO_3$ has been reported to arise from an excitation maximum at 330 nm.[19] In conclusion, the spectral features of CTi:*y* solids do not seem to be affected by the XRD phase present, although the latter are probably responsible for the differences observed in the luminescence intensities (Figs. 1, 3). This could imply a similarity in the luminescence mechanism operating across the CTi:*y* solids as a whole.

In contrast, the luminescence spectra of the CCr:*y* solids are somehow related to the XRD phases detected in them. In fact, some differences are observed clearly in the spectra of the above solids, depending on whether the CaO phase is detectable or not in all the samples. Thus, although the total luminescence intensity decreases progressively with addition of Cr to CaO, the spectral features of the CCr:0.5–10 solids are similar to those of pure CaO. Clearly, chromium addition results also in an enhanced contribution of the blue–green emission, even at 0.5% addition [Fig. 2(a)]. However, the blue emission from CCr:0.5–30 solids produced by excitation at 200 nm is clearly associated with the CaO phase, present in all of them, and not to their chromium content since first, the spectral features are similar to those of pure CaO and secondly the chromium addition quenches the total luminescence intensity.

On the other hand, luminescence in the CCr:30–100 solids is very weak and arises mainly from the excitation near 240 nm instead of 200 nm, as well as from a third distinct excitation state, near 220 nm, which is absent for the CCr:0.5–10 solids (Fig. 4). These features are probably related to the chromium present but it is not our purpose to discuss them here. In any event, the weak luminescence that has been observed from the $CaCrO_4$ at low temperatures[20] is quite different from the luminescence of the CCr:*y* ($y \neq 0$) solids.

In conclusion, the luminescence spectral features of CTi:*y* ($y \neq 0$) and CCr:0.5–30 solids are similar to those of pure CaO, in spite of the differences observed in the total emission as well as in the relative band intensities. Although there are also some differences in the position of the emission bands maxima across spectra of the above solids, we conclude that the emission originates from centres of a similar nature in each case. This similarity suggests also a similarity in the nature of the photoprocesses involved for the CTi:*y* and CCr:0.5–30 solids as a whole.

Luminescence of CaO in air has been discussed in detail already in ref. 9 and was ascribed to radiative recombination processes. Briefly, according to the simplified model proposed, excitation of CaO by high-energy UV light can induce the formation of electron and hole states in the solid. The emission is a result of recombination processes between the photogenerated electrons and holes. These processes proceed through oxygen anion vacancies, with the intermediate formation of F^+ and F centres.[9] A similar photoluminescence mechanism is also possibly operational in the case of the CTi:*y* ($y \neq 0$) and CCr:0.5–30 solids, although the transition-metal cations involved may affect the salient processes in a certain way.

For CTi:0.5–70 and CCr:0.5–30 solids especially, where the CaO phase is detectable by XRD (Table 1), photo-effects obtained should be attributed to this phase, although the influence of the transition-metal ions present should be taken into account. This is supported by the present results, since the luminescence spectra of the above solids are quite similar to that of pure CaO, in spite of the variety of other XRD phases that are detected (Table 1). However these phases, in particular the transition-metal ions they contain, are probably responsible for the differences observed in the luminescence intensity of the solids.

The negative influence of the transition-metal ions on the photoluminescence intensity of the above solids could well be understood by considering their indirect participation in the photoprocesses taking place. According to the model proposed in ref. 9, the metal ions are neither excited nor emit themselves, although they can participate in the photoprocesses by changing their oxidation state, *viz.* $M^{n+} + e \rightleftharpoons M^{n-1+}$.

In fact, the electrons released from the valence band during the excitation, could be trapped initially by the transition-metal ions present, which then will change their oxidation state. If the transition-metal ions involved are strong acceptors, the photogenerated electrons will be strongly held by these and can not recombine with holes, so that the emission process will be hindered and the total luminescence intensity will be decreased. On the other hand, if the metal ions are able to accept electrons and therefore are converted to unstable cations, the emission process will proceed easily through the oxygen anion vacancies. Thus, as results from the photoluminescence mechanism considered, the total luminescence intensity should be defined primarily by the concentration of the oxygen anion vacancies present in the solids, but the facile establishment of the $M^{n+} + e \rightleftharpoons M^{n-1+}$ equilibrium during the UV irradiation is also important.

Therefore, the strong luminescence quenching observed across the CCr:0.5–30 solids [Fig. 5(b)], could be ascribed to

the influence of the chromium (probably Cr^{5+} or Cr^{3+}) cations present. The latter act as strong traps for the photogenerated electrons, thus hindering the recombination processes proceeding through the oxygen anion vacancies present. Then, the systematic diminution of the photoluminescence intensity in Fig. 5(b), seems to reflect the luminescence dependence from the concentration of chromium cations present.

In relation to the CTi:*y* solids, we note that their luminescence behaviour appears roughly to be determined by either the CaO phase (CTi:0.5–50), or the TiO_2 phase (CTi:50–100). The Ti^{4+}, or the Ca^{2+} cations, appear to decrease the CaO, or the TiO_2 luminescence, respectively [Fig. 5(a)]. The luminescence quenching effect of the titanium cations is smaller than that of chromium cations [Fig. 5(a) and (b)], possibly because of the stability of the $3d^0$ electronic configuration. The Ti^{4+} cations can trap electrons and be converted into Ti^{3+} donors, which in turn can easily be converted back to Ti^{4+}, thus releasing electrons to the oxygen vacancies present.

It has been reported,[9] that the recombination processes occurring in CaO through the F^+ centres results in blue or violet emission, while these occurring through the F centres give blue–green or green emission. Thus, the dominant emission from the solid, blue or green, should be defined by the direction of the equilibrium: $F \rightleftharpoons F^+ + e$ encountered in the illuminated solid. This balance is probably affected by the type and concentration of metal cations present, therefore the luminescence behaviour of the CTi:*y* ($y \neq 0$) and the CCr:0.5–30 solids should be defined by the combined equilibrium: $M^{n+} + F \rightleftharpoons M^{n-1+} + F^+$. Thus, if this equilibrium is somehow moves to the left, blue–green or green emission from the solid dominates, while if it is moves to the right, blue or violet emission is dominant.

Relation between catalytic activity and photoluminescence

As was mentioned in the introductory part of this work, a relation has been observed between the luminescence and the catalytic activity of the CZn:*y* solids for N_2O decomposition.[8] The linear relation existing between the reaction rate and the blue emission intensity, suggests the involvement of the F^+ centres in the catalytic mechanism for these solids.[8] It would be also of interest to search for a possible role of defect centres in the case of the CTi:*y* and the CCr:*y* solids, especially those rich in Ca, which certainly appeared to be active in the probe reaction examined here (Table 2).

Clearly, the blue emission component is not always the main one in the emission spectra of the CTi:*y* and CCr:*y* catalysts, in contrast to CZ:*y* catalysts.[8] In fact, the blue–green emission component clearly dominates for CCr:*y* ($y \neq 0$) catalysts (Fig. 2) and also seems to be dominant for CTi:30–70 catalysts (Fig. 1). However, as the CaO phase appears to be responsible for the photo-effects obtained from the catalysts (CTi:0.5–70 and CCr:0.5–30), we believe that a correlation between the catalytic activity and the blue emission intensity could possibly also hold here.

We observe that such a correlation does exist across each series of catalysts, CTi:*y* and CCr:*y*, examined separately, although CaO, as well as CTi:70 solids deviate from the apparent linear relationship between *R* and photoluminescence intensity. Thus, although a relation between the catalytic activity and the luminescence intensity is also expected to hold across the CTi:0.5–50 and the CCr:0.5–30 solids as a whole, and such a statistical linear relation is actually observed ($R^2 = 0.853$), we believe that the deviations in the slopes and ordinates of the particular straight lines are not accidental. They suggest rather different effects for different metal ions present in each solid series.

The above mentioned linear relationships suggest an analogy between the concentrations of the catalytically active sites for the N_2O decomposition and those of the F^+ type defects formed in each series of the catalysts during UV irradiation.[2] The fact that these relations are obtained although different conditions were used for the measurement of the two parameters, implies that the concentrations of the F^+ centres formed in the catalytic conditions for each catalytic series should be analogous to the corresponding concentrations of the F^+ type defects formed in the solids during UV irradiation at room temperature.

Therefore, CaO seems to deviate negatively from the relationships obtained, probably because the catalytic activity of the remainder of the CM:*y* solids is higher than that suggested by their photoluminescence intensity. This could be a result of the luminescence quenching caused by the transition-metal ions present. Thus, the distance, α, of the CaO point from each line obtained, parallel to the PL intensity axis, could be a measure of the competitive quenching action of the titanium or chromium ions towards photoluminescence.

We propose that, during the catalytic processes, the competitive action of the transition-metal ions towards F^+ centre formation through oxygen anion vacancies, disappears. Then, all of the vacancies present in the catalysts should participate in the $M^{n+} + F \rightleftharpoons M^{n-1+} + F^+$ equilibrium. As a result, the concentrations of the F^+ centres present under the catalytic conditions should be larger than those present in the solids during UV irradiation. No obstruction of the photoprocesses through oxygen anion vacancies seems to occur at room temperature over pure CaO or the CTi:70 solid, as their deviations from the linear relationships drawn permit us to presume. Then, the luminescence intensities measured in these cases correspond to the concentration of the F^+ centres also formed under the catalytic conditions. If so, the number of F^+ centres formed in both cases will be equal to the number of oxygen anion vacancies present in the solids.

If the above considerations are valid, the true value of F^+ centre concentration, across the CTi:0.5–50 and CCr:0.5–30 solids during the catalytic measurements, should correspond to a new, corrected value of the luminescence intensity, PL_{corr}, instead of the measured PL value, so that: $PL_{corr} = PL + \alpha$, where α measures the competitive action of the titanium or chromium ions towards photoluminescence, as noted above. As a result, a new improved linear relation ($R^2 = 0.953$) is obtained between the catalytic activity and the corrected photoluminescence intensity across the CM:*y* (M = Ti, Cr) catalysts as a whole (Fig. 6). Therefore the catalytic, as well as the photoluminescence processes over our solids, appear to proceed through the oxygen anion vacancies, especially through the F^+ type defects formed.

The role of F^+ centres in chemisorption over irradiated CaO is well known.[21,22] The possibility of the influence of the

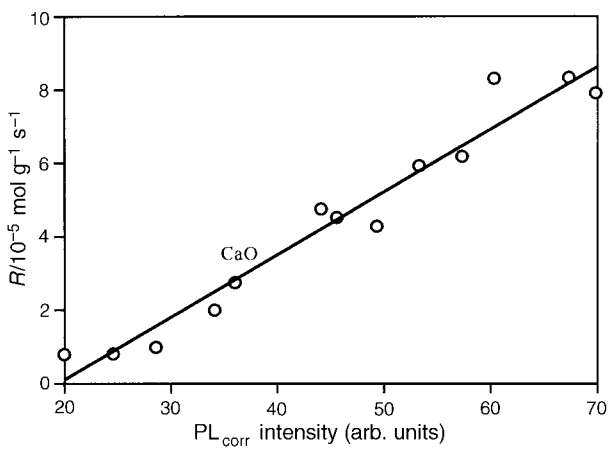

Fig. 6 Relation between the catalytic activity for N_2O decomposition at 550 °C and the corrected photoluminescence of the CM:*y* catalysts (M = Ti or Cr, *y* = 0.00–70 or 0.00–30 respectively)

F^+ and F type defects on the catalytic activity of the solids has been ignored in most catalytic studies, although their involvement in catalysis has been assumed previously.[7,23–28] More specifically, these defects may act as the active electron-donor centres for N_2O decomposition over the simple oxides.[7,23–25] The arguments of the discussion given above, strengthened by the inferences of the kinetic analysis presented previously, confirm the role of the F^+ type defects in the catalysts examined here. To be more precise, the F^+ centres are the electron donors for the activated adsorption of N_2O on CM : y (M = Ti, Cr) catalysts, according to step (I) in the N_2O decomposition reaction route.

Therefore, the electron-transfer processes that facilitate catalytic N_2O decomposition, proceed on the solids examined here through oxygen anion vacancies, with the intermediate formation of F^+ type defects. The reaction rate is possibly defined by the $M^{n+} + F \rightleftharpoons M^{n-1+} + F^+$ equilibrium in the solids under catalytic conditions. Obviously, the establishment of such a balance requires the existence of non-stoichiometry, of oxygen deficiency type, in the prepared solids, probably here as a result of their treatment during preparation.

In conclusion, although the catalytic activity for N_2O decomposition and the luminescence intensity of the pure CaO are affected in different ways by addition Ti or Cr, a relation between the two parameters has been established across the range of the $(CaO)_{1-x}(MO)_x$ (M = Ti, Cr) catalysts studied. The present results strengthen the proposition that the F^+ type defects play a significant role in catalytic N_2O decomposition on oxide systems containing CaO.

References

1 A. Cimino, *Chim. Ind*., 1974, **56**, 27.
2 J. C. Vickerman, *Spec. Per. Rep. Catal. II*, 1979, 107.
3 P. Pomonis and J. C. Vickerman, *J. Catal*., 1978, **55**, 88.
4 P. Pomonis and J. C. Vickerman, *J. Catal*., 1984, **90**, 305.
5 S. Louis Rai and V. Srinivasan, *J. Catal*., 1980, **65**, 121.
6 L. G. Tejuca and J. L. G. Fierro, *Adv. Catal*., 1989, **36**, 237.
7 H. H. Kung, *Transition Metal Oxides: Surface Chemistry and Catalysis*, Elsevier, Amsterdam, 1989.
8 L. A. Loukatzikou, A. T. Sdoukos and P. J. Pomonis, *Catal. Lett*., 1996, **41**, 113.
9 L. A. Loukatzikou, A. T. Sdoukos and P. J. Pomonis, *J. Mater. Chem*., 1996, **6**, 887.
10 Ch. Kordulis, L. Vordonis, A. Lykourgiotis and P. Pomonis, *J. Chem. Soc., Faraday Trans. 1*, 1987, **83**, 627.
11 P. Pomonis, Ch. Kordulis and A. Lykourgiotis, *J. Chem. Soc., Faraday Trans*., 1990, **86**, 711.
12 Ch. Kordulis, H. Latsios, A. Lykourgiotis and P. Pomonis, *J. Chem. Soc., Faraday Trans*., 1990, **86**, 185.
13 E. R. S. Winter, *Discuss. Faraday Soc*., 1959, **28**, 183.
14 K. V. Ramanujachary and C. S. Swamy, *J. Catal*., 1985, **93**, 279.
15 L. G. J. De Haart and G. Blasse, *J. Solid State Chem*., 1986, **61**, 135.
16 A. Amtout and R. Leonelli, *Solid State Commun*., 1992, **84**, 349.
17 M. Anpo, *Res. Chem. Intermed*., 1989, **11**, 67.
18 M. Anpo, M. Tomonari and M. A. Fox, *J. Phys Chem*., 1989, **93**, 7300.
19 M. Wiegel, M. Hamoumi and G. Blasse, *Mater. Chem. Phys*., 1994, **36**, 289.
20 G. A. M. Dalhoeven and G. Blasse, *Chem. Phys. Lett*., 1980, **76**, 27.
21 R. L. Nelson, A. J. Tench and B. J. Harmsworth, *Trans. Faraday Soc*., 1967, **63**, 1427.
22 R. L. Nelson and A. J. Tench, *Trans. Faraday Soc*., 1967, **63**, 3039.
23 E. R. S. Winter, *J. Catal*., 1969, **15**, 144.
24 E. R. S. Winter, *J. Catal*., 1970, **19**, 32.
25 K. V. Ramanujachary, N. Kameswari and C. S. Swamy, *J. Catal*., 1984, **86**, 121.
26 Ming-Cheng Wu, C. M. Truong, K. Coulter and D. W. Goodman, *J. Am. Chem. Soc*., 1992, **114**, 7565.
27 Ming-Cheng Wu, C. M. Truong, K. Coulter and D. W. Goodman, *J. Catal*., 1993, **140**, 344.
28 A. G. Anshits, E. N. Voskresenskaya and L. I. Kurteeva, *Catal. Lett*., 1990, **6**, 67.

Paper 6/08609H; *Received* 24*th December*, 1996